Production of silver-doped analcime by isomorphous substitution technique

B. Kwakye-Awuah,* I. Radecka, M. A. Kenward and C. D. Williams*

Research Centre in Applied Sciences, University of Wolverhampton, Wolverhampton, WV1 1SB, UK

Abstract

BACKGROUND: Metal-exchanged zeolites have been reported to have significant limitations on cayalytic activity, such as counterbalancing the negative framework charges and limitation of active space. Alternative methods of incorporating silver ions into the framework of zeolites are therefore necessary. This paper reports on a technique for producing silver doped analcime by isomorphous substitution of silver ion into the framework of analcime. The amount of aluminium in the gel composition was reduced by a factor of 5%, 10% and 20% and an equivalent amount of silver was added to the gel and treated in a conventional manner for zeolite crystallisation. Some of the aluminium in the reaction gel was replaced with the silver. The silver-doped analcime samples where characterised by X-ray diffraction (XRD), scanning electron microscopy (SEM), energy dispersive X-rays (EDX), Fourier transform infrared (FTIR) spectroscopy and inductively coupled plasma-atomic emission spectroscopy (ICP-AES) analysis.

RESULTS: The amount of silver ions loaded for each reduction of aluminium as determined by EDX were found to be (w/w) 0.29%, 1.41% and 2.10%, respectively. XRD pattern SEM images of the silver-doped analcime showed the presence of zeolite P in addition to analcime.

CONCLUSION: Silver-doped analcime was successfully produced with different silver loadings and may exhibit higher anti-microbial activities than silver-exchanged counterparts.

Keywords: analcime; silver-doped analcime; isomorphous substitution; characterisation

INTRODUCTION

Analcime ($NaAlSi_2O_6.H_2O$) is a mineral belonging to the tectosilicate group with a zeolitic structure of a complex aluminosilicate framework.[1] However, new examinations have shown that, depending on conditions and type of impurities present, natural analcime may belong to cubic, tetragonal, orthorhombic, monoclinic or triclinic crystallographic systems. It is well known that analcime is a potential precursor for a new generation of dental porcelains having high fracture resistance.[2,3] Previous work by Ueda and Koizumi showed that analcime can form from a clear aqueous solution.[4] In the laboratory, analcime is readily synthesized under hydrothermal conditions. In recent years heavy metals (in particular transition metals) have been substituted within the framework of many zeolites by ion exchange with the mobile charge balancing cations within the zeolite framework.[5] These metal-exchanged zeolites can exhibit high antimicrobial activity.[6,7] In comparison with other antimicrobial heavy metals, silver in the form of silver ions is the most common metal incorporated into zeolite frameworks for use in reducing microbial contaminations. This is because silver and silver ions are relatively less toxic to humans and exhibit a broad spectrum of antimicrobial activity at low concentrations.[6] Metal-exchanged zeolites have the following limitations: (1) loading is restricted to counterbalancing the negative framework charge; (2) the pore system becomes partially blocked upon the introduction of ion-exchanged transition metals, which in turn limits the active space for catalytic conversion;[2] (3) the ion exchange method results in surface deactivation and is a time-consuming multistep experimental procedure; (4) metal cation mobility and undesirable chemical reactivity often results.[8] Because of such limitations it is essential to anchor the silver ions on both external and internal surfaces of the zeolites so that when it comes into contact with a microorganism the silver ions can effectively inhibit microbial growth.[6,7] To achieve such objectives the silver ions must be substituted with the mobile cation isomorphously. Very recently, the influence of the chemical properties of aluminium-containing components and preparation conditions of γ-Al_2O_3 on the crystal system of analcime, formed under hydrothermal conditions, has been analyzed.[5] This paper reports on the synthesis and characterization of silver doped analcime under hydrothermal conditions. This was done by

* Correspondence to: B. Kwakye-Awuah and C.D. Williams, Research Centre in Applied Sciences, University of Wolverhampton, Wolverhampton, WV1 1SB, UK

E-mail: a.kwakyeawuah@wlv.ac.uk; C.Williams@wlv.ac.uk

(*Received 15 November 2007; revised version received 16 January 2008; accepted 4 February 2008*)

Published online 14 April 2008; DOI: 10.1002/jctb.1938

 J Chem Technol Biotechnol 0268–2575/2008/$30.00

reducing the aluminium composition in the reaction gel and adding equivalent silver ions to obtain a silver-doped analcime. The silver-doped analcime was characterized according to its structure, surface morphology, chemical composition, particle size distribution and its structural features.

MATERIALS AND METHOD

Materials

Sodium hydroxide was purchased from Aldrich Chemicals, UK, kaolinite from ECC international in Cornwall, UK, sodium silicate from Fischer Chemicals, UK, and the de-ionized water used in this investigation was supplied by University of Wolverhampton.

Synthesis of silver-doped analcime

The starting sols were made according to the reaction gel composition, $6.5Na_2O{:}Al_2O_3 : 4.5SiO_2 : 380H_2O : 6.1$: triethanolamine (TEA),[1] with some modifications; kaolinite was used as aluminium source. 9.8 g of kaolinite was first dissolved in 55 g of distilled water. Simultaneously, 14.9 g of sodium silicate (dissolved in 36.5 g distilled water) was mixed with 12.2 g of triethanolamine. The kaolinite solution and silicate solution were mixed together under constant stirring for 15 min. Thoroughly homogenized synthesis mixtures were treated hydrothermally in a Teflon-lined stainless steel autoclave at 200 °C for 24 h. After the hydrothermal treatment, the content of the autoclave was washed with 1 L distilled water, vacuum filtered and dried in an electric oven at 100 °C. The supernatant was transferred to a conical flask and analyzed by inductively coupled plasma-atomic emission spectroscopy (ICP-AES). Silver doped-analcime was prepared as follows: 1 mol L^{-1} silver nitrate solution (1.96 g in 10 mL distilled water) was pre-added to 9.31 g of kaolinite solution to obtain about 5% reduction of aluminium in the kaolinite. The molar composition of the silicate and TEA were unaltered. The silicate–TEA and the silver kaolinite solutions were mixed with constant stirring until a homogeneous solution was obtained. The content was hydrothermally treated and crystallized in the same conventional manner as before. Silver-doped analcime with aluminate reduction of 10% and 20% were prepared by pre-adding 2 mol L^{-1} silver nitrate solution (3.92 g in 10 mL distilled water) and 4 mol L^{-1} silver nitrate solutions (7.84 g in 10 mL distilled water) and repeating the synthesis procedure.

Characterization of silver-doped analcime

X-ray diffraction

The phase purity of silver-doped analcime particles was analyzed with X-ray diffraction (XRD). The diffraction patterns were recorded on a Philips PW 1710 X-ray powder diffractometer over a 2θ range 3° to 50°. The diffractometer was equipped with a graphite monochromated Cu K_α radiation source (8978 eV; $\lambda = 1.5418$ Å). Portions of the analcime samples were placed on the flat auto-plate and pressed down to fill the entire perimeter of the plate using a glass plate. After obtaining a smooth and level powder surface, the plates were stacked on an auto-stand. A proportion of the X-rays were diffracted by the regular crystal structure of the samples.

Morphological analysis by scanning electron microscopy (SEM)

The surface morphologies of both zeolites were examined by SEM, using a Zeiss EVO 50 (Zeiss, UK).

Energy dispersive X-ray (EDX) analysis

The chemical compositions of both zeolites were determined by EDX (Oxford Instruments, UK). EDX was also used to determine the concentration of silver ions in the analcime crystals. An area scan was taken over four different regions and the mean concentration (with standard deviations) was calculated.

Particle size distribution

The particle size and surface area distributions per unit volume were analyzed using a Mastersizer X long bed analyzer (Malvern Instruments, UK).

Fourier transformed infrared (FTIR) spectroscopy

FTIR spectroscopy of the undoped and silver-doped analcime was carried out to investigate the structural features of the analcime. The analysis was performed with a Mattson FTIR (Thermo, Cambridge, UK) spectrometer with a durasope. The measurements were over 100 scans and a wave number range 400–4000 cm^{-1}.

Inductively coupled plasma-atomic emission spectroscopy (ICP-AES)

The percentage of silver ions in the supernatant was determined by (ICP-AES) (SPECTRO, UK). The intensity of radiation is proportional to the concentration of the element within the sample and is shown directly as a percentage or measured concentration.

RESULTS

XRD analysis

XRD spectra of undoped and of 5%, 10% and 20% silver-doped analcime samples are shown in Fig. 1. Highly crystalline particles were obtained for all loadings and for the control (undoped analcime). This is verified by SEM images (Fig. 2). The doping of analcime with Ag^+ resulted in 0.2° shift of the peaks to the right for 20% silver loading although the crystalinity of the crystals was retained. The peak intensities were not reduced, indicating that there were no carbonaceous materials present in the analcime crystals.[5,9] Traces of zeolite P were identified (Fig. 1) at 11.5°, 22° and 23°. These peaks can be considered to represent a

J Chem Technol Biotechnol **83**:1255–1260 (2008)
DOI: 10.1002/jctb

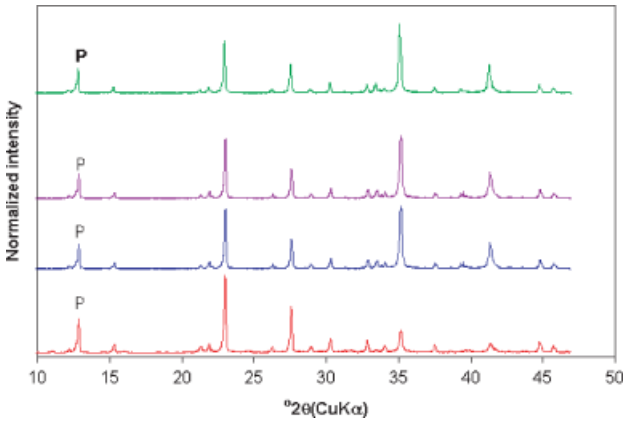

Figure 1. XRD spectra – all loadings.

metastable phase, which converts to analcime over time.[5]

SEM analysis

The SEM micrographs of undoped and doped analcime are shown in Fig. 2. The morphology of the particles showed both cubic and spherical shapes[5] for both the undoped analcime and for all loadings, with average size between 10 and 20 µm. There were small crystals in between the analcime particles for undoped analcime and for 5%, 10% and 20% silver-doped analcime. The source of these small crystals is not clear but can be attributed to the initial formation of analcime that was suppressed during the crystallization process.[9,10] This can also be seen in the XRD spectra (Fig. 1) where the peak patterns were narrower than the undoped analcime.

EDX analyses

The EDX spectra detected the presence of silver ions for all loadings (Fig. 3). The loadings were higher for a 20% (w/w) substitution of Ag^+. The spectra also show the presence of Ag^+. This is verified by the results of the X-ray microanalysis shown in Table 2. The gold peak (marked by an arrow) detected in the spectrum was due to the a gold coating of the sample prior to analysis. No Ag^+ was detected for the undoped analcime (Table 1). The EDX also quantified the amount of Ag^+ trapped within the analcime framework (cavities or the exchangeable sites). An amount of 0.285% (w/w) of Ag^+ was either trapped within the analcime structure or at the exchangeable sites upon 5% (w/w) substitution of Ag^+. 1.41% (w/w) was trapped within the cavities or at the exchangeable sites with 10% Ag^+ with equivalent substitution of Ag^+, and 2.09% (w/w) was trapped within the cavities or at the exchangeable sites upon 20% (w/w) substitution of Ag^+. As a result there was 19% (w/w) aluminium reduction on doping with 5% Ag^+, 47% (w/w) aluminium reduction on doping with 10% Ag^+ and 53% aluminium reduction on doping with 20% Ag^+ (Table 2).

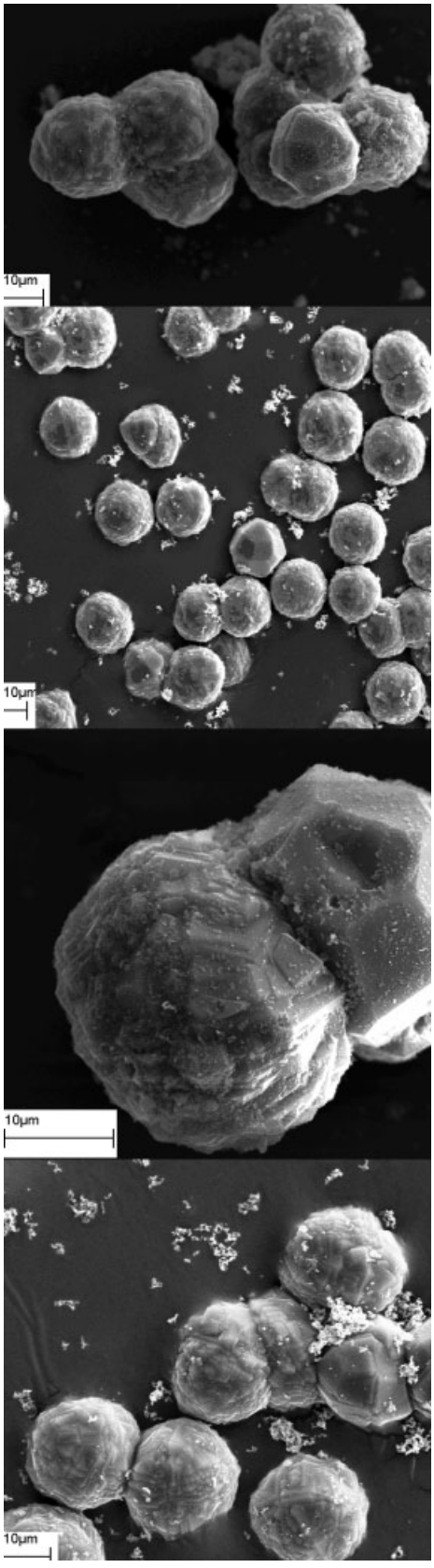

Figure 2. SEM micrographs – all loadings.

Particle size distribution

Figure 4 shows the distribution of undoped analcime particles and analcime doped with Ag^+. The sizes of the zeolite particles were not the same. The modal

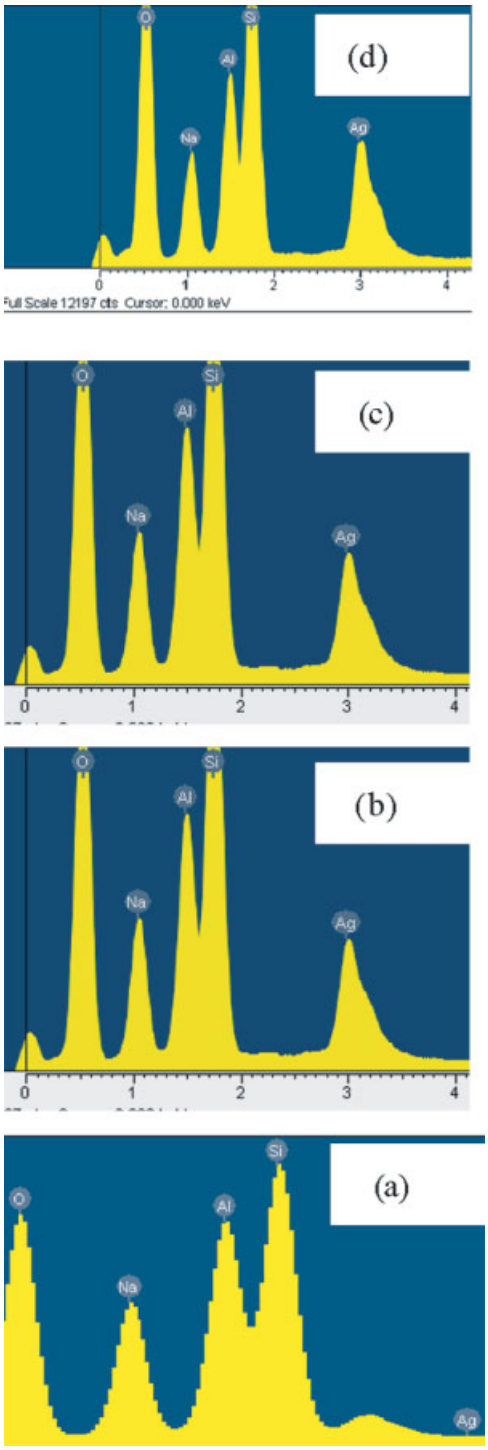

Figure 3. Analcime, 0–20% Ag loading.

Table 2. Amount of Ag^+ detected in the supernatant (ICP-AES) for undoped analcime and for various loadings of Ag^+

Percentage aluminate reduction	[Ag^+] in supernatant (ppm)
0	0.00
5	3.86
10	7.46
20	27.90

distribution of the particles occurred at 23 μm for undoped and 5% Ag^+-doped analcime, and 2.0 μm for 10% and 20% Ag^+-doped analcime.

FTIR analysis

Results obtained for the FTIR analysis are shown in Fig. 5. In general, FTIR spectroscopy can give information concerning structural details of the material.[8,11] Two groups of vibrations are associated with FTIR spectroscopy: *internal vibrations* of framework TO_4 units which are insensitive to structural vibrations and *vibrations relating to the external linkage* of the TO_4.[9,11,12] Although each zeolite has a characteristic FTIR pattern some common features are observed for all zeolites.[12] The FTIR spectrum for undoped analcime is shown in Fig. 5(a). The main band centered at 1026 cm^{-1} is attributed to the asymmetric stretching of the Si–O and Al–O belonging to the SiO_4 and AlO_4 tetrahedra.[9,11] The corresponding internal bending modes of the Si–O–Al bonds give rise[1,12,13] to a transmission band at 426 cm^{-1}. Moreover, three bands were detected in the 500–800 cm^{-1} region. The first and second occurred at 598 cm^{-1} and 622 cm^{-1}, respectively. Both bands are narrow and exhibit the lowest relative intensity. The third one occurred at 728 cm^{-1} and is broader than the others. According to Mozgawa[13] these bands can be attributed to the external vibration modes of the SiO_4 tetrahedra producing the over-tetrahedra form of the zeolite middle range order.[9] In the case of analcime, these bands are attributed to the external vibrations of the four-membered double rings (4DR) and the six-membered single rings (6SR) units, respectively.[13] The bands centered at 888 cm^{-1} and 917 cm^{-1} are attributed to the asymmetric stretching mode of the Si–O–Al bonds.[1,13] On doping the analcime with 5% Ag^+ (Fig. 5(b)) there was no change in the spectrum (with reference to the absorption bands of the starting

Table 1. EDX analysis of elemental composition with various loadings of silver ions into the analcime framework ($n = 4$)

	Weight (%) ± stdev*				Atomic weight (%)			
Element	0% Ag^+ loading	5% Ag^+ loading	10% Ag^+ loading	20% Ag^+ loading	0% Ag^+ loading	5% Ag^+ loading	10% Ag^+ loading	20% Ag^+ loading
O	42.08 ± 0.14	46.20 ± 0.12	56.93 ± 0.13	56.78 ± 0.12	54.36	59.32	71.11	72.72
Na	14.79 ± 0.08	11.86 ± 0.06	9.73 ± 0.07	8.97 ± 0.06	13.3	10.62	8.44	7.96
Al	17.17 ± 0.08	13.88 ± 0.05	9.13 ± 0.06	8.10 ± 0.05	13.15	10.57	6.75	6.15
Si	26.12 ± 0.1	26.19 ± 0.06	17.38 ± 0.07	15.19 ± 0.06	19.22	19.55	12.36	11.08
Ag	0.00 ± 0.01	1.89 ± 0.10	6.83 ± 0.09	10.99 ± 0.10	0.00	0.36	1.41	2.09

* stdev = standard deviation

J Chem Technol Biotechnol **83**:1255–1260 (2008)
DOI: 10.1002/jctb

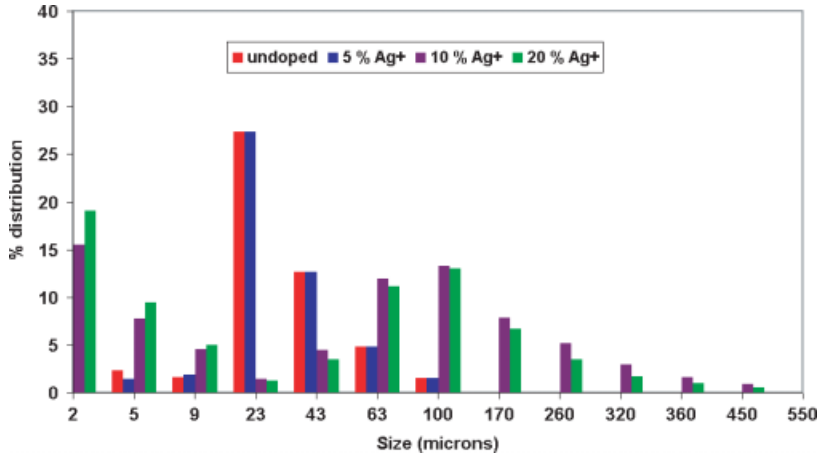

Figure 4. Particle size with and without Ag.

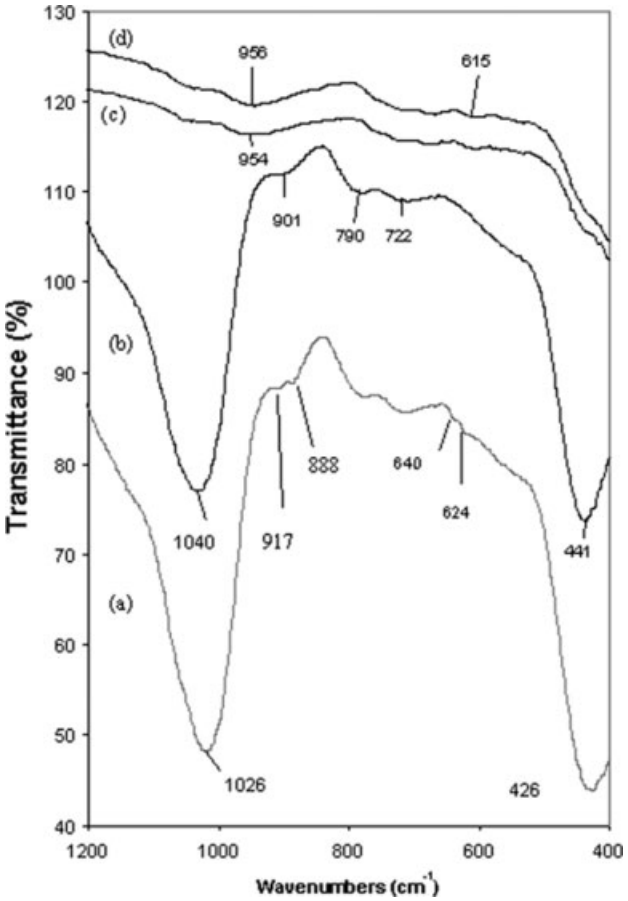

Figure 5. FTIR of analcime – all loadings.

analcime) with the exception of the band centered at 888 cm^{-1}, which was reduced significantly. Further doping (10% and 20%) of Ag^+ resulted in the loss of bands at 1026 cm^{-1} and 426 cm^{-1} in each case and the peak intensities of the remaining bands were significantly reduced.

ICP-AES analysis

Results obtained for the ICP-AES analysis are shown in Table 2. Ag^+ ions were not detected in the supernatant of the undoped analcime. Ag^+ ions were detected in minute quantities in the supernatant compared with the amount trapped in the analcime framework (Table 2). Doping a portion of the analcime by 5% Ag^+ resulted in 2.86 ppm of Ag^+ present in the supernatant. The Ag^+ concentration almost doubled on doping the starting analcime by 10%, while doping with 20% Ag^+ resulted in 27.90 ppm of Ag^+ present in the supernatant (approximately three times compared with 5% doping with Ag^+).

DISCUSSION

Silver-doped analcime was successfully synthesized for the first time in the laboratory (Fig. 1). Ag^+ ions were detected as verified by the EDX spectra (Fig. 3). SEM analysis confirms that the crystallographic structure of undoped analcime is icositetrahedral, while a cubic structure was obtained for all loadings. Since the sizes of the particles were not the same, the surface area of the zeolite was also different (Fig. 4). The particle size per volume of the particles showed two peaks when doped with Ag^+ which were not present in the case of the undoped analcime. It is known that the symmetric and asymmetric stretching modes of the Si–O and Al–O bonds with n bridging oxygen (where n is the number of Si–O or Al–O tetrahedra) are IR active in the 800–1300 cm^{-1} range with the Si–O bonds stronger than the Al–O bonds.[1,3,14] Consequently, the isomorphous substitution of the Al atoms with a transition Ag^+ replaced some of the Al atoms within the framework of the analcime. This is confirmed by the results obtained from the elemental composition (Table 1). It is known that the Ag–O bonds (around 995 cm^{-1}) are weaker than the Al–O bonds.[12] There is no evidence of such bond formation from the FTIR spectra (Fig. 5). The main absorption bands on doping the analcime with 10% and 20% Ag^+ are centered at lower values of 954 cm^{-1}, 956 cm^{-1} and 850 cm^{-1} (Fig. 5(c), 5(d)) instead of absorption bands at 1200, 1100, 950, 900 for undoped analcime (Fig. 5(a)). This can be attributed to the shielding provided by Ag^+ due to the isomorphous substitution.

It is therefore likely that some bonds were unable to vibrate completely. The XRD patterns (Fig. 1) show the shift in diffraction peaks when doped with Ag^+. The fact that the crystalinity of the structures was not altered implies that the 4DR and 6DR rings were unaffected by the presence of Ag^+.[15] This can confirm that Ag^+ was trapped within the framework including the exchangeable sites. The position of the IR ring bands depend on the Si:Al ratio and the degree of ring deformation.[11,16] The decrease in the number of ring members shifts the characteristic bands towards higher wave numbers.[11] In this work, however, there is no evidence of such a shift as the main absorption bands are lower (Fig. 5(c), 5(d)). From the FTIR spectra (Fig. 5) the following findings are evident:

(1) Doping the analcime with a lower amount of Ag^+ (Fig. 5(b)) did not cause changes to the internal and external stretching modes. The amount of Ag^+ trapped within the analcime framework (Table 1) is 0.285% (w/w). This demonstrates that analcime can tolerate doping at this concentration;
(2) Doping the analcime with higher amounts of Ag^+ (Fig. 5(c), 5(d)) resulted in 1.41% and 2.10% (w/w) being trapped in the framework with a significant reduction of most absorption bands. These observations suggest that the analcime structure (particularly the 4DR and 6SR members) were unable to vibrate as a result of the level of Ag^+ doping. However, it is worth noting that the results from XRD, SEM and/or particle size analysis are not consistent with this suggestion.

CONCLUSION

Silver-doped analcime was produced for the first time in the laboratory. The stretching of the Si–O–Al bonds did not affect the crystalinity of the analcime framework although significant stretching of the bonds was observed. To date silver-exchanged zeolites have been produced both industrially and in the laboratory by ion-exchange methods. The limitations associated with this approach have been ignored or overlooked. An alternative route to transition metal-exchanged zeolites is recommended. The technique used in this study for the production of silver-doped analcime can be used as a model to produce different silver-doped zeolites and these can exhibit excellent anti-microbial activity.

ACKNOWLEDGEMENTS

The authors are grateful to the University of Wolverhampton for funding this work

REFERENCES

1 Novotna M, Satava V, Lezal D, Klouzkova A and Kostka P, Preparation and characterisation of analcime powders. *J Optoelect Adv Mater* **5**:S1405–S1409 (2003).
2 Giampaolo C and Lombardi G, Thermal behaviour of analcimes from two different genetic environments. *Eur J Mineral* **6**:285–289 (1994).
3 Line CMB, Putnis A, Putnis C and Giampaolo C, The dehydration kinetics and microtexture of analcime from two parageneses. *Am Mineral* **80**:268–279 (1995).
4 Ueda S and Koizumi M, Crystallization of mordenite from aqueous solutions. *Am Mineral* **64**:172–179 (1979).
5 Ballands A and Traidaraite A, The influence of Al containing component of synthesis of analcime of various crystallographic systems. *Mater Sci-Pol* **25**:(2007).
6 Matsumura Y, Yoshikata K, Kunisaki S and Tsuchido T, Mode of action of silver zeolite and its comparison with that of silver nitrate. *Appl Environ Microbiol* **69**:4278–4281 (2003).
7 Brett DW, A discussion of silver as an antimicrobial agent: Alleviating the confusion. *Ostomy/Wound Man* **52**(1):34–41 (2006).
8 Van Bekkum H, Flanigen EM, Jacobs PA and Jansen JC, Introduction to zeolite science and practice, in *Studies in Surface Science and Catalysis*, ed. by Van Bekkum H, Flanigen EM, Jacobs PA and Jansen JC. Elsevier Science Publishers, Amsterdam, **137**, 469–472 (2001).
9 Kohoutková M, Kloužková A, Maixner J and Mrázová M, Preparation and Characterization of Analcime Powders by X-ray and SEM Analyses. *Ceramics-Silikáty* **51**(1):9–14 (2007).
10 Kloužková A, Mrázová M and Kohoutková M, Synthesis of partially stabilised leucite. *J Phys Chem Sol* **68**:1207–1210 (2007).
11 Aronne A, Esposito S and Pernice P, FTIR and DTA study of lanthanum aluminosilicate glasses. *Mater Chem Phys* **51**:163 (1997).
12 Sitarz M, Handke M and Mozgawa W, FTIR studies of the cyclosilicate-like structures. *J Mol Struct* **596**(1-3):185–189 (2001).
13 Mozgawa W, The relation between structure and vibrational spectra of natural zeolites. *J Mol Struct* **596**:129–137 (2001).
14 Gruciani G and Gualtieri A, Dehydration dynamics of analcime by in situ synchrotron powder diffraction. *Am Mineral* **84**:112 (1999).
15 Seok HL, Yang K and Karl S, Weak Ag^+–Ag^+ bonding in zeolite X. Crystal structures of $Ag_{92}Si_{100}Al_{92}O_{384}$ hydrated and fully dehydrated in flowing oxygen. *J Microporous Mesoporous Mater* **41**(1-3):49–59 (2000).
16 Hovis GL, Roux J and Rodrigues E, Thermodynamic mixing properties of nepheline-kalsilite crystalline solutions. *Am Mineral* **87**:1108–1127 (2002).